System-size effects at the isotropic-nematic transition from computer simulation

Enrique de Miguel
Departamento de Física Atómica, Molecular y Nuclear, Universidad de Sevilla, Apartado 1065, Sevilla 41080, Spain
(Received 11 September 1992)

We present a computer-simulation study regarding the effect of system size on the isotropic-nematic transition in a molecular fluid model. Systems of 256, 500, and 864 molecules interacting through the Gay-Berne model are analyzed along an isotherm by using molecular dynamics in the *NVT* ensemble. For the three system sizes under consideration, the system exhibits a weak first-order isotropic-nematic transition. The transition densities are calculated by using thermodynamic integration. We find that the transition shifts to higher densities as the number of particles N increases. In addition, the transition weakens as N gets larger. These results are used to extract information on the transition properties in the infinite-system limit. The N dependence of thermodynamic properties are estimated from the simulation results and are compared with theoretical predictions.

PACS number(s): 64.70.Md, 05.70.Fh, 61.25.Em

I. INTRODUCTION

One of the final aims in computer simulation of condensed matter is to obtain information on the macroscopic behavior of a system. One is obviously limited by the fact that any realistic simulation has to be performed by considering small samples of the system under consideration. It would be then desirable to know how to extrapolate the various properties obtained for small systems to the infinite-size sample. In addition, it is well established that the finite size of the simulated sample introduces systematic deviations from the bulk (infinite) behavior [1–3]. These finite-size effects are expected to be particularly noticeable at phase transitions. It has not been until recently that phenomenological theories combined with Monte Carlo simulations [1–5] have addressed the study of finite-size effects at first-order transitions.

The main signature of any first-order transition is the discontinuity in the first derivatives of the free energy. This results in δ-function singularities in the susceptibility and specific heat of the system. Due to finite size of the system what is rather observed is a finite peak at the singularities [4,5]. As reported for field- and temperature-driven first-order transitions [4,5], this rounding takes place with peak height increasing as V and half-width decreasing as V^{-1}, where V is the volume of the sample (for a given number density N/V the relevant scaling variable can be either V or the number of particles of the system N; in what follows we shall use N for convenience). Another effect related with finite N values is that the location of the transition is expected to be shifted from the bulk value. As recognized elsewhere [5], this shift is not fully understood, though an N^{-1} dependence is expected.

In the case of classical fluids there is still some controversy on the extent of the N dependence of the thermodynamic properties of a simulated system. Even though a certain system-size dependence close to a phase transition is generally claimed, the situation is less clear when the simulation deals with fluids far from the transition. For instance, while Guillot and Guissani [6] report that the chemical potential of the Lennard-Jones fluid depends on N, others [7] claim that this dependence is rather weak. A recent work by Smit and Frenkel [8] does indeed show that the excess chemical potential measured by the Widom particle-insertion method exhibits a strong N dependence. Moreover, these authors make a quantitative estimation of the corrections to the chemical potential predicting an N^{-1} dependence. Due to the fact that these corrections increase with the density of the system, care should be taken as to whether phase transitions that take place in the high-density region are still present in the infinite-system limit. For instance, Zarragoicoechea, Levesque, and Weis [9] have reported a Monte Carlo study of hard ellipsoids showing that for prolate 3:1 molecules the system exhibits a significant system-size dependence. These authors claim that for systems of 256 molecules, the nematic phase seems not to be stable between the isotropic and the solid phase. This behavior is to be compared with that shown for systems of 108 molecules where the nematic phase is indeed stable [10].

In the present work we address the study of finite-size effects arising in the isotropic and nematic phases of a molecular model by molecular-dynamics computer simulation. It is well established that the isotropic-nematic (I-N) transition, which implies the onset of long-range orientational order, is weakly first order as found experimentally and from computer simulation [9–12]. Most computer simulations on this subject show that, regardless of the particular nature of the model under consideration, the density (or volume) change at the I-N transition amounts to approximately 2%. This value, however, is larger than that usually reported for real nematic liquid crystals ($\approx 0.5\%$). This discrepancy is usually ascribed to the small samples which have to be simulated due to computing-time limitations. One might expect a closer agreement between simulation and real experiment as the size of the simulated system goes to infinity. Evidently, if other factors, such as molecular flexibility, polarizability, or biaxiality, were explicitly

considered in the models, one would also expect a better quantitative agreement with experiments.

In this work we locate the I-N transition for systems with $N=256$, 500, and 864 molecules interacting via the Gay-Berne model [13]. This potential can be regarded as a generalization of the spherically symmetric Lennard-Jones potential to uniaxial ellipsoidal particles with axial ratio $a:b$. This model fluid has been shown to exhibit nematic behavior for the particular elongation 3:1 at sufficiently high densities and temperatures [12,14,15]. By using thermodynamic integration [16] we show that for the elongation 3:1 the nematic phase is stable for the three system sizes investigated. As said above, this is by no means evident.

The remaining part of the paper is arranged as follows: In Sec. II we present in some detail the thermodynamic-integration method. We then proceed in Sec. III to show the computer-simulation results for the different values of N. The I-N transition densities are calculated and the system-size effects for the Gay-Berne fluid are studied. In Sec. IV these results are analyzed in the light of theoretical predictions regarding the N dependence of the chemical potential. In Sec. V we summarize this work and present its main conclusions.

II. THERMODYNAMIC INTEGRATION METHOD

Let us consider a system made up by N molecules enclosed in a volume V. Let us consider two state points characterized by their number density ρ and ρ_0. The thermodynamic-integration method allows the calculation of the difference in free energy between these two states from knowledge of the pressure of the system along a reversible path linking both states. If these states are connected through an isotherm one has the following relation:

$$\frac{F_N(\rho)}{Nk_BT}=\frac{F_N(\rho_0)}{Nk_BT}+\int_{\rho_0}^{\rho}\frac{P_N(\rho')}{\rho' k_BT}\frac{d\rho'}{\rho'} , \tag{1}$$

where k_B is the Boltzmann's constant, T is the temperature, and F_N and P_N are the Helmholtz free energy and pressure of the N-particle system (for finite systems, these quantities depend on N). It becomes clear that, in order to calculate $F_N(\rho)$, we need to have at our disposal (a) the equation of state $P_N(\rho)$, and (b) the free energy of the reference-state point $F_N(\rho_0)$. The reference-state point should be chosen such that its free energy is known or easily calculable.

For the isotropic phase, we chose the ideal-gas limit as reference state. In such a case, it is easy to show that the free energy at any isotropic (i) density is given by

$$\frac{F_N^i(\rho)}{Nk_BT}=\frac{F_N^{\mathrm{id}}(\rho)}{Nk_BT}+\int_0^{\rho}\left[\frac{P_N^i(\rho')}{\rho' k_BT}-1\right]\frac{d\rho'}{\rho'} , \tag{2}$$

where $P_N^i(\rho)$ is the equation of state of the isotropic fluid and $F_N^{\mathrm{id}}(\rho)$ is the (analytically known) free energy of N linear rotors in the ideal-gas limit.

The free energy of the nematic (n) phase is obtained by direct application of Eq. (1):

$$\frac{F_N^n(\rho)}{Nk_BT}=\frac{F_N^n(\rho_0^n)}{Nk_BT}+\int_{\rho_0^n}^{\rho}\frac{P_N^n(\rho')}{\rho' k_BT}\frac{d\rho'}{\rho'} , \tag{3}$$

where $P_N^n(\rho)$ is the equation of state along the nematic branch of the isotherm. It should be noticed that in this case there is not a direct reversible path linking the low-density (ideal-gas) limit and the nematic phase because a discontinuous phase transition has to be crossed. As a consequence, we cannot consider the ideal gas as the reference-state point as done for the isotropic phase. In order to calculate the free energy of the nematic reference-state point $F_N^n(\rho_0^n)$, we consider the Gay-Berne fluid in an external field represented by the Hamiltonian

$$H_{\mathrm{ext}}(\lambda)=\lambda\sum_{i=1}^{N}\sin^2\theta_i , \tag{4}$$

where λ is the strength of the field and θ_i is the angle between the axial unit vector of molecule i and the (arbitrary) direction of the external field. Notice that, for sufficiently strong fields, the effect of (4) on the system is to align molecules along the direction of the field, i.e., a nematic phase can be artificially stabilized even for densities at which an isotropic behavior is expected in the absence of the field [10,12,17]. Proceeding in this way, we can reversibly connect an ideal gas of oriented molecules with the nematic reference-state point ρ_0^n without crossing any phase transition. Let λ_0 be a strength value for which the I-N transition is effectively suppressed and consider the following reversible path: (i) Switch on the external field at constant density $\rho=0$ from $\lambda=0$ to λ_0; (ii) compress the (nematic) Gay-Berne fluid at constant external field λ_0 from $\rho=0$ to the nematic density of interest ρ_0^n; and (iii) switch off the external field at constant density ρ_0^n from $\lambda=\lambda_0$ to 0. The change in free energy along this artificial path will enable us to compute the free energy of the nematic reference-state point $F_N^n(\rho_0^n)$ in Eq. (3). It can be shown [12] that

$$\frac{F_N^n(\rho_0^n)}{Nk_BT}=\frac{F_1}{Nk_BT}+\frac{F_2}{Nk_BT}+\frac{F_3}{Nk_BT} , \tag{5}$$

with

$$\frac{F_1}{Nk_BT}=-\ln\left[\exp(-\beta\lambda_0)\sum_{m=0}^{\infty}\frac{1}{2m+1}\frac{(\beta\lambda_0)^m}{m!}\right] , \qquad \beta=\frac{1}{k_BT} \tag{6}$$

being the external-field contribution in the ideal-gas limit,

$$\frac{F_2}{Nk_BT}=\frac{F_{\lambda_0}^{\mathrm{id}}(\rho_0^n)}{Nk_BT}+\int_0^{\rho_0^n}\left[\frac{P_N^{\lambda_0}(\rho')}{\rho' k_BT}-1\right]\frac{d\rho'}{\rho'} , \tag{7}$$

being the free energy change in the compression process in the presence of the external field, and

$$\frac{F_3}{Nk_BT}=\frac{-1}{Nk_BT}\int_0^{\lambda_0}d\lambda\left\langle\sum_{i=1}^{N}\sin^2\theta_i\right\rangle_{\rho} \tag{8}$$

being the change in free energy when the external field is turned off. The angular brackets in Eq. (8) indicate an

ensemble average. The free energy of the nematic reference point is finally obtained by adding up Eqs. (6)–(8). When this value is at our disposal, the free energy of the nematic phase is readily calculated from integration of the nematic equation of state in Eq. (3).

III. COMPUTER SIMULATION RESULTS

We have performed molecular-dynamics (MD) simulations at constant number of particles (N), volume (V), and temperature (T) for Gay-Berne fluids. According to the Gay-Berne model [13], the intermolecular pair potential is given by

$$U_{12}(r,\hat{\mathbf{r}},\hat{\mathbf{u}}_1\hat{\mathbf{u}}_2)=4\varepsilon(\hat{\mathbf{r}},\hat{\mathbf{u}}_1,\hat{\mathbf{u}}_2)\left\{\left[\frac{\sigma_0}{d(\hat{\mathbf{r}},\hat{\mathbf{u}}_1,\hat{\mathbf{u}}_2)}\right]^{12}-\left[\frac{\sigma_0}{d(\hat{\mathbf{r}},\hat{\mathbf{u}}_1,\hat{\mathbf{u}}_2)}\right]^{6}\right\}, \tag{9}$$

with $d(\hat{\mathbf{r}},\hat{\mathbf{u}}_1,\hat{\mathbf{u}}_2)=r-\sigma(\hat{\mathbf{r}},\hat{\mathbf{u}}_1,\hat{\mathbf{u}}_2)+\sigma_0$, where r is the distance between the centers of mass of molecules 1 and 2. The angular dependence is set in the potential through the range and energy parameters which are given, respectively, by

$$\sigma(\hat{\mathbf{r}},\hat{\mathbf{u}}_1,\hat{\mathbf{u}}_2)=\sigma_0\left\{1-\frac{\chi}{2}\left[\frac{(\hat{\mathbf{r}}\cdot\hat{\mathbf{u}}_1+\hat{\mathbf{r}}\cdot\hat{\mathbf{u}}_2)^2}{1+\chi(\hat{\mathbf{u}}_1\cdot\hat{\mathbf{u}}_2)}+\frac{(\hat{\mathbf{r}}\cdot\hat{\mathbf{u}}_1-\hat{\mathbf{r}}\cdot\hat{\mathbf{u}}_2)^2}{1-\chi(\hat{\mathbf{u}}_1\cdot\hat{\mathbf{u}}_2)}\right]\right\}^{-1/2}, \tag{10a}$$

$$\varepsilon(\hat{\mathbf{r}},\hat{\mathbf{u}}_1,\hat{\mathbf{u}}_2)=\varepsilon_0[1-\chi^2(\hat{\mathbf{u}}_1\cdot\hat{\mathbf{u}}_2)^2]^{-1/2}\times\left\{1-\frac{\chi'}{2}\left[\frac{(\hat{\mathbf{r}}\cdot\hat{\mathbf{u}}_1+\hat{\mathbf{r}}\cdot\hat{\mathbf{u}}_2)^2}{1+\chi'(\hat{\mathbf{u}}_1\cdot\hat{\mathbf{u}}_2)}+\frac{(\hat{\mathbf{r}}\cdot\hat{\mathbf{u}}_1-\hat{\mathbf{r}}\cdot\hat{\mathbf{u}}_2)^2}{1-\chi'(\hat{\mathbf{u}}_1\cdot\hat{\mathbf{u}}_2)}\right]\right\}^{2}, \tag{10b}$$

with $\chi=(\kappa^2-1)/(\kappa^2+1)$ and $\chi'=(\kappa'^{1/2}-1)/(\kappa'^{1/2}+1)$, where κ is the molecular length-to-breadth ratio and κ' is the ratio of the potential-well depths for the side-by-side and end-to-end configurations.

It should be noticed that for $\kappa=\kappa'=1$, the Gay-Berne potential reduces to the Lennard-Jones potential with $\sigma=\sigma_0$ and $\varepsilon=\varepsilon_0$. In what follows, we will consider σ_0 and ε_0 as length and energy units. The simulations reported here were performed by considering the anisotropy parameters $\kappa=3$ and $\kappa'=5$.

The reduced temperature ($T^*=k_BT/\varepsilon_0=1.25$) was kept constant by scaling the molecular velocities step by step [18]. For this particular temperature, we have already shown [12] that a system of 256 Gay-Berne particles undergoes a first-order transition from the isotropic to the nematic phase. Molecules were considered as linear rigid rotors with no rotational motion about the main symmetry axis and with a moment of inertia $I^*=I/m\sigma_0^2=1$. The equations of motion were numerically integrated by using a Gear predictor-corrector method considering a time step $\Delta t^*=0.0015$ with $\Delta t^*=\Delta t(m\sigma_0^2/\varepsilon_0)^{1/2}$.

For the three system sizes investigated, $N=256$, 500,864, we have basically followed the same procedure employed in Ref. [12]. In all cases, the potential was cut and shifted at a distance $r_c^*=r_c/\sigma_0=4.0$. As a time-saving device, we made use of a neighbor list. The simulation box was cubic and usual periodic boundary conditions were used. Initially, molecules were placed on an fcc lattice at very low density [$\rho^*=(N/V)\sigma_0^3=0.02$]. After a few hundred time steps, the lattice structure melted, forming a translationally disordered fluid. The corresponding final configuration was then slowly compressed in small density jumps ($\Delta\rho^*=0.01$) always starting from the previous equilibrated configuration. At each density, the system was first allowed to equilibrate over approximately 10 000 time steps and averages were afterwards collected over 10 000–15 000 additional time steps.

To monitor the onset of orientational order, we followed the behavior of the order parameter S_2 along the isotherm. This quantity is defined as the simulation average of the largest eigenvalue of the Q tensor [11]:

$$Q_{\alpha\beta}=\frac{1}{N}\sum_{i=1}^{N}\left(\tfrac{3}{2}u_\alpha^i u_\beta^i-\tfrac{1}{2}\delta_{\alpha\beta}\right), \tag{11}$$

where u_α^i ($\alpha=x,y,z$) is the Cartesian component of the axial unit vector of molecule i. Values of the order parameter as obtained from the simulations are included in Table I for the three system sizes under consideration. These values are plotted in Fig. 1 against the reduced density. It can be seen that at low densities the system remains orientationally disordered. The values of the order parameter, however, are not exactly zero as would be expected for an isotropic phase. It can be shown [19] that for a finite system, S_2 fluctuates around an average value of the order of $1/N$: only in the thermodynamic limit does the order parameter reach the expected zero value. At intermediate densities ($\rho^*\approx0.25$), order-

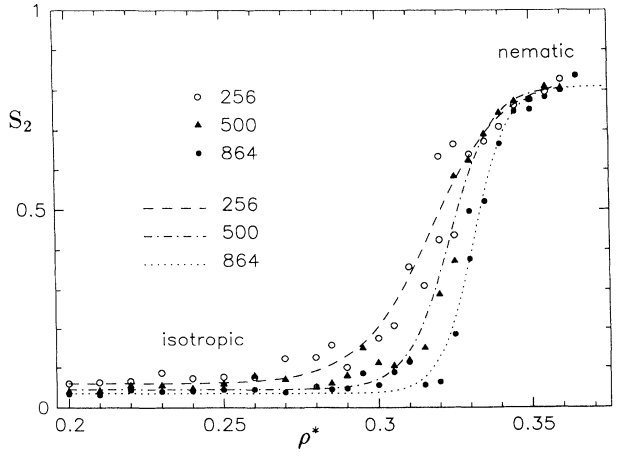

FIG. 1. Orientational order parameter S_2 as obtained from molecular-dynamics computer simulation for systems of 256, 500, and 864 Gay-Berne molecules in the neighborhood of the isotropic-nematic transition at the reduced temperature $T^*=1.25$. Lines have been included as a fit of the simulation data. Density is expressed in reduced units $\rho^*=\rho\sigma_0^3$.

TABLE I. Molecular-dynamics results for the orientational order parameter S_2 along the isotherm $T^*=1.25$ for the Gay-Berne fluid with elongation 3:1 for three system sizes $N=256$, 500, and 864 molecules.

ρ^*	$S_2(N=256)$	$S_2(N=500)$	$S_2(N=864)$
(a) Isotropic phase			
0.200	0.060	0.041	0.034
0.210	0.064	0.043	0.032
0.220	0.066	0.055	0.044
0.230	0.087	0.055	0.041
0.240	0.074	0.049	0.042
0.250	0.077	0.060	0.046
0.260	0.076	0.080	0.046
0.270	0.123	0.071	0.039
0.280	0.126	0.051	0.053
0.285	0.159	0.061	0.046
0.290	0.100	0.080	0.049
0.295		0.151	0.086
0.300	0.177	0.112	0.057
0.305	0.208	0.104	0.089
0.310	0.358	0.119	0.114
0.315	0.311	0.151	0.057
0.320	0.325	0.289	0.065
0.325	0.336	0.372	0.227
0.330			0.227
(b) Nematic phase			
0.325	0.666	0.624	0.521
0.330	0.641	0.643	0.577
0.335	0.673	0.690	0.631
0.340	0.709	0.744	0.667
0.345	0.762	0.772	0.747
0.350	0.777	0.776	0.752
0.355	0.797	0.809	0.783
0.360	0.827	0.805	0.800

parameter fluctuations become more sluggish and averages larger than $1/N$ are obtained. These fluctuations become more evident for smaller system sizes. Upon further compressing the isotropic fluid, a sudden increase in the order parameter is observed. This fact is associated with an orientational disorder-order transition. The high-density phase was identified as a nematic fluid after noticing that the molecular centers of mass remained translationally disordered above the transition while the molecular orientations displayed a well-defined average direction of alignment. For each N-molecule system, this preferential direction was different. This fact makes us to believe that the periodic boundary conditions play no role in stabilizing the nematic phase.

From Fig. 1 we can infer that the isotropic-nematic transition shifts to slightly higher densities as the system is larger. In addition, it seems that the pretransition region, where anomalously large order-parameter values are found, extends over a wider range of densities for smaller systems.

Values of the reduced pressure $P^*=P\sigma_0^3/\varepsilon_0$ are presented in Table II. In Fig. 2 the equation of state of the Gay-Berne fluid is shown along the isotherm $T^*=1.25$. It can be observed that the onset of orientational

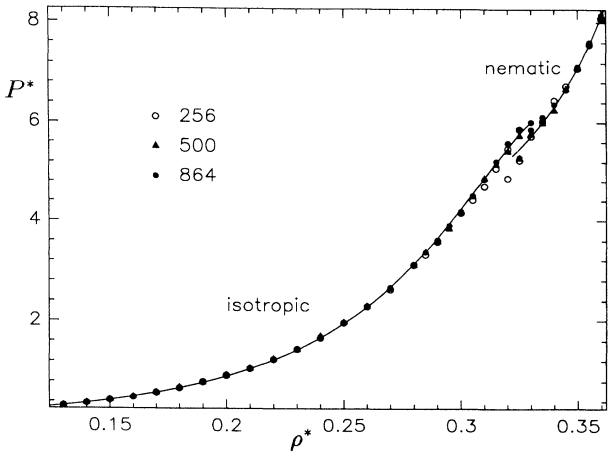

FIG. 2. Equation of state of the Gay-Berne fluid with $\kappa=3$, $\kappa'=5$ as obtained from molecular-dynamics computer simulation for systems of 256, 500, and 864 molecules along the isotherm $T^*=1.25$. The continuous line corresponds to the equation of state in the infinite-size limit obtained from extrapolation of the simulation data (see text). Pressure and density are expressed in reduced units $P^*=P\sigma_0^3/\varepsilon_0$ and $\rho^*=\rho\sigma_0^3$, respectively.

TABLE II. Molecular-dynamics results for the pressure $P^*=P\sigma_0^3/\varepsilon_0$ along the isotherm $T^*=1.25$ for the Gay-Berne fluid with elongation 3:1 for three system sizes $N=256$, 500, and 864 molecules.

ρ^*	$P^*(N=256)$	$P^*(N=500)$	$P^*(N=864)$
(a) Isotropic phase			
0.200	0.920	0.918	0.903
0.210	1.052	1.051	1.063
0.220	1.233	1.241	1.232
0.230	1.438	1.429	1.434
0.240	1.660	1.692	1.684
0.250	1.958	1.965	1.954
0.260	2.287	2.290	2.274
0.270	2.629	2.645	2.666
0.280	3.115	3.100	3.097
0.285	3.319	3.374	3.372
0.290	3.603	3.584	3.569
0.295		3.840	3.902
0.300	4.158	4.174	4.191
0.305	4.418	4.488	4.506
0.310	4.699	4.859	4.845
0.315	5.069	5.151	5.212
0.320	5.472	5.419	5.583
0.325	5.863	5.731	5.869
0.330			6.007
(b) Nematic phase			
0.325	5.241	5.283	5.293
0.330	5.722	5.760	5.856
0.335	6.020	5.989	6.111
0.340	6.448	6.247	6.367
0.345	6.731	6.673	6.659
0.350	7.088	7.089	7.130
0.355	7.567	7.580	7.671
0.360	8.086	8.078	8.136

order in the system is accompanied by a discontinuity in the density of the fluid. This is what we expect from a system undergoing a first-order transition.

The simulations were implemented on a CONVEX C-240 computer. No optimization scheme was attempted for the computer code and double precision was used for all calculations. The time required for each state point depended on the total number of particles and the number density. Typically, at a reduced density $\rho^*=0.320$ (close to the isotropic-nematic transition), the CPU time for the 256-, 500-, and 864-particle system was 0.35, 0.66, and 1.14 sec per step, respectively. Occasionally, a DECstation 5000/200 computer was used. In this case, the required CPU time was greater than the CONVEX C-240 time approximately by a factor of 1.5.

A. Location of the I-N transition

Due to the first-order nature of the I-N transition, the values of the transition densities cannot be directly extracted from the MD results. In the case of the I-N transition, where the transition involves the onset of long-range orientational order, a natural way to locate approximately the transition is to follow the behavior of the orientational order parameter S_2. However, a mere estimate of the transition densities from Fig. 1 does not seem to be the best way to proceed if the displacement of the transition due to system-size effects needs to be quantified. The most reliable method for calculating the transition densities involves the evaluation of the free energy of the coexisting phases. In this work we have used thermodynamic integration for determining the absolute free energies $F_N^i(\rho)$ and $F_N^n(\rho)$ for a system of N Gay-Berne particles in the isotropic (i) and nematic (n) phases following the scheme presented in Sec. II.

For the implementation of the thermodynamic integration, a suitable parametrization of the equations of state is needed. This was performed by fitting the corresponding simulation pressures in terms of a y expansion:

$$P^*=\frac{2}{\pi}\sum_{m=1}^{M} A_m y^m , \tag{12}$$

with $y=x/(1-x)$, x being the packing fraction. The coefficients A_m were calculated by standard linear least-squares fit [20]. The degree of the fitting polynomial M was chosen such that the χ^2 of the fitting was not essentially reduced after considering higher orders. The isotropic pressures were well represented by considering $M=6$ while for the nematic pressures, a value $M=3$ was considered. The equation of state of the Gay-Berne fluid when the external field is applied was represented by a similar expansion with $M=6$. The fitting coefficients for the different system sizes and phases have been collected in Table III.

Once the absolute free energy of the isotropic and nematic phases has been calculated, the chemical potential of both phases can be directly obtained from the relation

$$\frac{\mu_N(\rho)}{k_BT}=\frac{F_N(\rho)}{Nk_BT}+\frac{P_N(\rho)}{\rho k_BT} . \tag{13}$$

TABLE III. Fitting coefficients of the equation of state, Eq. (12), for Gay-Berne fluids with molecular shape 3:1 as obtained from molecular-dynamics simulation: (a) isotropic phase, (b) nematic phase, and (c) Gay-Berne plus external field.

	$N=256$	$N=500$	$N=864$
(a) Isotropic			
A_1^{iso}	1.2500	1.2500	1.2500
A_2^{iso}	0.9646	0.5590	0.2205
A_3^{iso}	4.9552	9.9202	13.1607
A_4^{iso}	6.8918	−10.8334	−21.2384
A_5^{iso}	−6.6399	17.4637	30.3511
A_6^{iso}	0.9622	−9.9848	−15.2794
(b) Nematic phase			
A_1^{nem}	−9.9936	12.0204	6.1137
A_2^{nem}	25.5064	−12.1220	−1.3978
A_3^{nem}	−7.9849	7.9770	3.2209
(c) External field			
A_1^{ext}	1.2500	1.2500	1.2500
A_2^{ext}	−0.0281	−0.0247	−0.0586
A_3^{ext}	5.7180	4.6433	4.7284
A_4^{ext}	−0.1245	4.0425	3.5698
A_5^{ext}	−0.0583	−5.1373	−4.2810
A_6^{ext}	−0.3706	1.5644	1.1352

The desired transition densities follow from the conditions for chemical and mechanical equilibrium (i.e., equality of pressures and chemical potentials of both phases). The transition densities so obtained for $N=256$-, 500-, and 865-particle systems are presented in Table IV, together with other thermodynamic properties at the I-N transition. A detail of the isotherm $T^*=1.25$ in the transition region is shown in Fig. 3 for the three

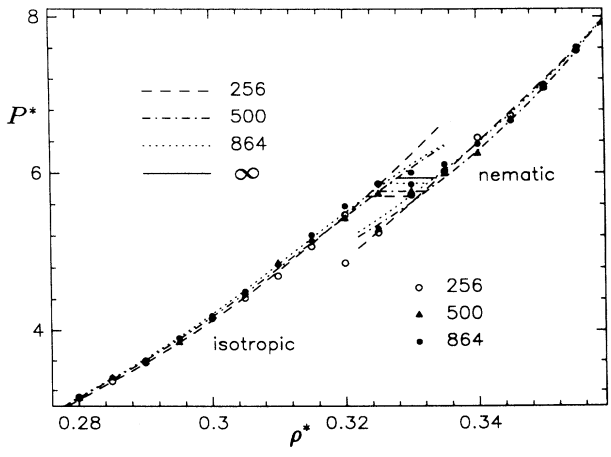

FIG. 3. Detail of the equation of state at the isotropic-nematic transition for the reduced temperature $T^*=1.25$. The coexistence densities for the different system sizes have been connected by horizontal lines. The horizontal continuous line indicates the location of the transition for the infinite-size system by assuming an N^{-1} scaling behavior of the coexistence densities at the transition.

TABLE IV. Coexistence properties at the isotropic-nematic transition for Gay-Berne fluids with molecular shape 3:1 along the isotherm $T^*=1.25$ for $N=256$, 500, and 864 molecules. Quantities have been expressed in reduced units: $\rho^*=\rho\sigma_0^3$, $P^*=P\sigma_0^3/\varepsilon_0$, and $\mu^*=(\mu-\mu^0)/k_BT$, with μ^0 being the temperature-dependent part of the ideal gas chemical potential. The relative density change at the transition is defined as $\Delta\rho_{IN}=(\rho_N^*-\rho_I^*)/\rho_N^*$.

N	ρ_I^*	ρ_N^*	$\Delta\rho_{IN}$	P_{IN}^*	μ_{IN}^*
256	0.3232	0.3311	0.0239	5.703	16.74
500	0.3251	0.3323	0.0217	5.767	16.90
864	0.3259	0.3325	0.0198	5.868	17.12
∞ [a]	0.3277	0.3338	0.0182	5.952	17.34
∞ [b]	0.3270	0.3332	0.0168	5.910	17.24

[a]Values obtained after solving the equilibrium conditions with P_∞^* and μ_∞^* (see text).

[b]Values obtained from extrapolation of the simulation transition densities by assuming a linear relation with N^{-1}.

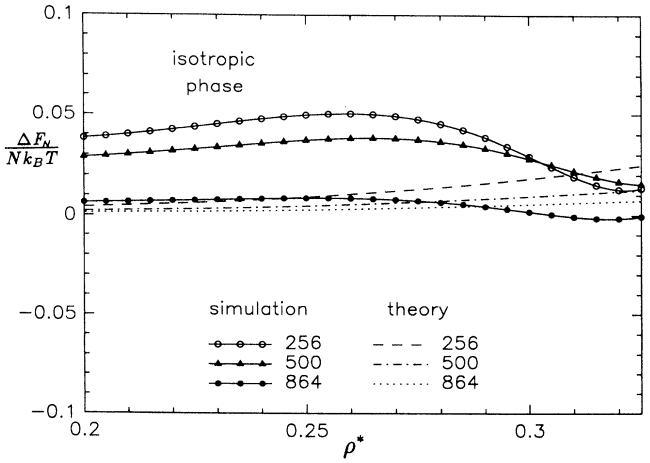

FIG. 5. Finite-size corrections to the free energy $\Delta F_N/Nk_BT$ as a function of the reduced density in the isotropic phase for the reduced temperature $T^*=1.25$. Symbols correspond to the corrections obtained from simulation. Lines correspond to the corrections predicted by Eq. (17).

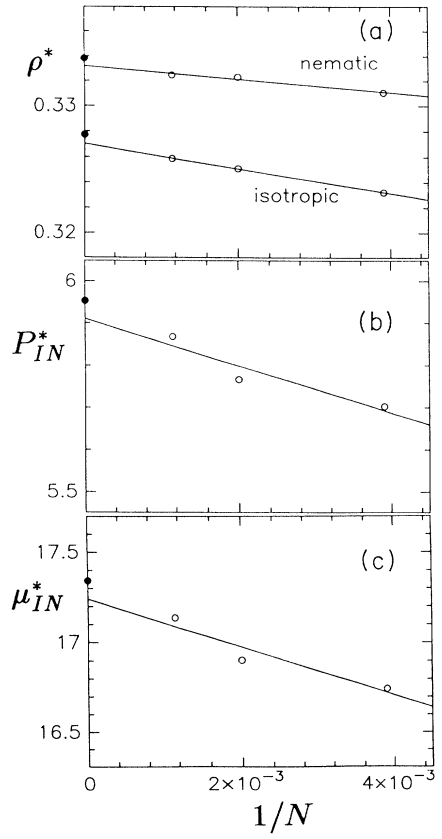

FIG. 4. Thermodynamic properties at the isotropic-nematic transition as a function of the inverse number of particles N^{-1} for the reduced temperature $T^*=1.25$: (a) nematic and isotropic coexistence densities; (b) pressure; (c) chemical potential. Filled dots correspond to the values obtained from solving the equilibrium conditions with $P_\infty^{\rm iso}$, $P_\infty^{\rm nem}$, $\mu_\infty^{\rm iso}$, and $\mu_\infty^{\rm nem}$ (see text).

system sizes. As expected from the behavior of the order parameter (see Fig. 1), the transition is effectively displaced to higher densities as the size of the system is increased.

B. System-size effects

The thermodynamic integration implemented above allows us to have the free energy (and hence the chemical potential and pressure) of the isotropic and nematic phases for the three finite systems. From these values, we have calculated at each density the corresponding value in the infinite-size limit $F_\infty(\rho)$ by assuming a linear

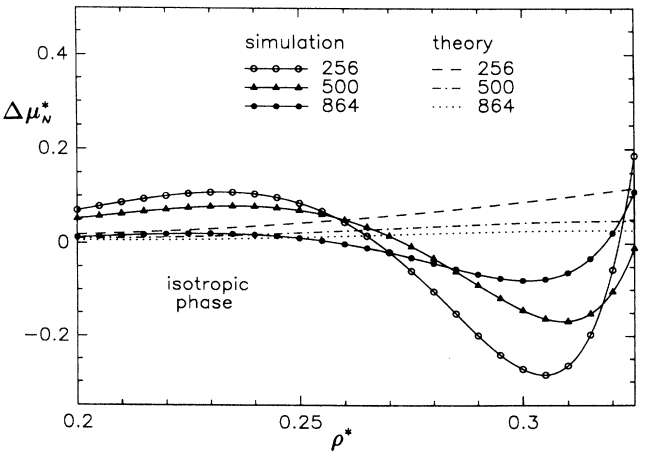

FIG. 6. Finite-size corrections to the chemical potential $\Delta\mu_N/k_BT$ as a function of the reduced density in the isotropic phase for the reduced temperature $T^*=1.25$. Symbols correspond to the corrections obtained from simulation. Lines correspond to the corrections predicted by Eq. (16).

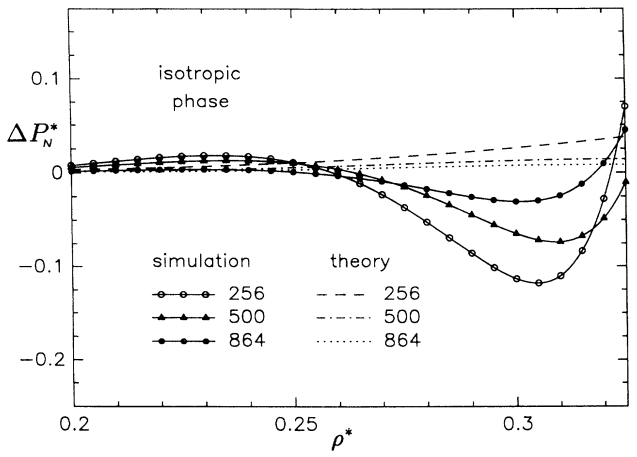

FIG. 7. Finite-size corrections to the pressure ΔP_N^* as a function of the reduced density in the isotropic phase for the reduced temperature $T^*=1.25$. Symbols correspond to the corrections obtained from simulation. Lines correspond to the corrections predicted by Eq. (18).

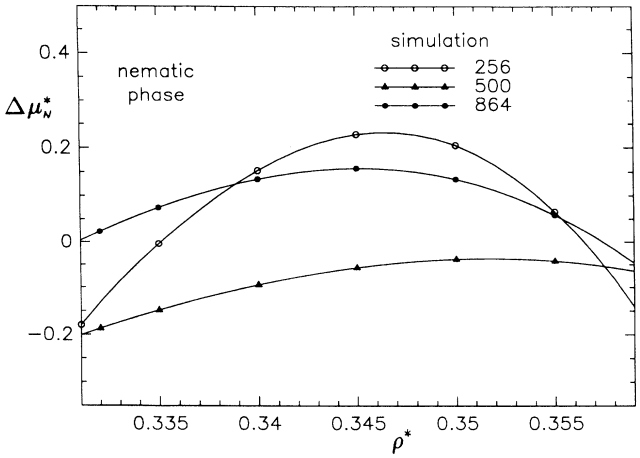

FIG. 9. Finite-size corrections to the chemical potential $\Delta\mu_N/k_BT$ free energy as a function of the reduced density in the nematic phase as obtained from simulation at the reduced temperature $T^*=1.25$.

behavior of $F_N(\rho)$, $\mu_N(\rho)$, and $P_N(\rho)$ with N^{-1} and then extrapolating to the limit $N^{-1}\to 0$. Even though this is the scaling behavior expected at the transition, there is no *a priori* reasons why this behavior should be also expected away from the transition. There are, however, analytical predictions concerning the N dependence of thermodynamic properties [8] that support this expection. This point will be considered in Sec. IV. We have not attempted any other scaling law of the type $N^{-\delta}$ with $\delta\neq 1$. Proceeding in this way, we have calculated the coexistence densities in the infinite-size limit by using the equilibrium conditions, but now using the extrapolated values of $\mu_\infty(\rho)$ and $P_\infty(\rho)$. The values so obtained are included in Table IV. In this table, we have also included the values of the coexistence densities obtained by assuming the same linear relation for the transition densities. We notice that these values seem to agree quite closely with those obtained from extrapolation of $\mu_\infty(\rho)$ and $P_\infty(\rho)$.

In Fig. 4 we present the coexistence densities, pressure, and chemical potential at the isotropic-nematic transition as a function of the inverse number of particles.

From the values of $F_\infty(\rho)$ we have calculated the simulation corrections to the corresponding finite-system values, defined as $\Delta F_N(\rho)=F_N^{\rm sim}(\rho)-F_\infty(\rho)$. Finite-size corrections to the chemical potential and pressure have been evaluated as well. These values are presented as a function of the reduced density in Figs. 5–7 for the isotropic phase and in Figs. 8–10 for the nematic region.

IV. COMPARISON WITH THEORETICAL PREDICTIONS

In this section we compare the simulation results presented in Sec. III with some expressions recently de-

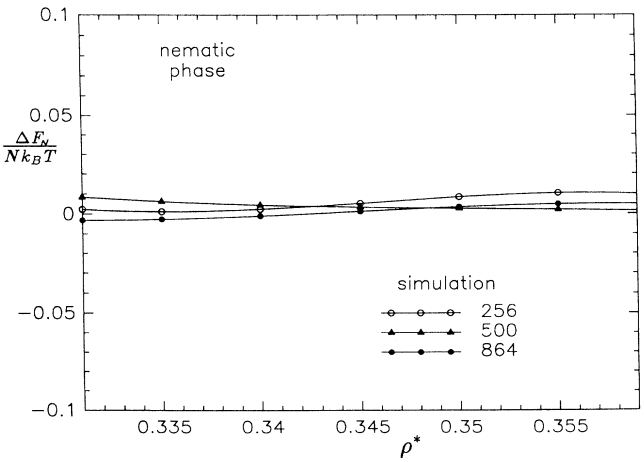

FIG. 8. Finite-size corrections to the free energy $\Delta F_N/Nk_BT$ as a function of the reduced density in the nematic phase as obtained from simulation at the reduced temperature $T^*=1.25$.

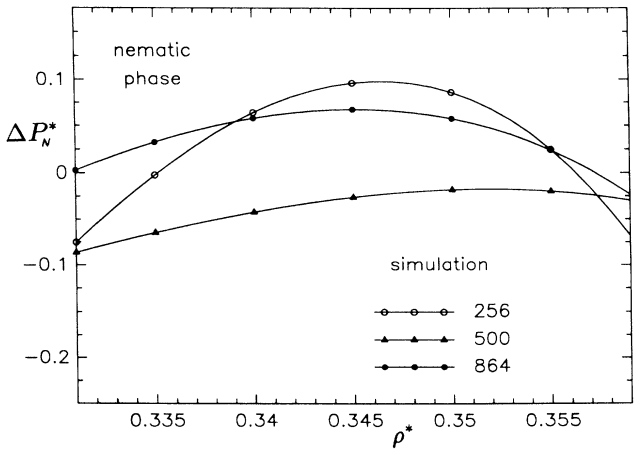

FIG. 10. Finite-size corrections to the pressure ΔP_N^* free energy as a function of the reduced density in the nematic phase as obtained from simulation at the reduced temperature $T^*=1.25$.

rived by Smit and Frenkel [8] for the finite-size corrections of thermodynamic quantities. In Ref. [8], it is shown that to leading order in $1/N$, the finite-size correction to the chemical potential is given by

$$\Delta\mu_N=\mu_N-\mu_\infty=\frac{1}{2N}\left[\frac{\partial P}{\partial\rho}\right]_{V,T}\left[1-k_BT\left[\frac{\partial\rho}{\partial P}\right]_{N,T}\right]^2, \tag{14}$$

where μ_N is the chemical potential for a system of N particles and μ_∞ the corresponding value for the infinite-size system. Due to the fact that all simulations reported here are performed at constant N, Eq. (14) cannot be directly tested. However, as noted in Ref. [8], Eq. (14) can be manipulated so as to obtain a more suitable expression. From the thermodynamic relation

$$\left[\frac{\partial\rho F}{\partial\rho}\right]_{N,T}=N\mu \tag{15}$$

it follows that the corresponding finite-size corrections to the free energy ΔF_N is given by

$$\left[\frac{\partial\rho\Delta F_N}{\partial\rho}\right]_{N,T}=N\Delta\mu_N\ . \tag{16}$$

After noticing that at $\rho=0,\Delta F_N=0$, the value of ΔF_N at any density follows from integration in Eq. (16):

$$\frac{\Delta F_N(\rho)}{Nk_BT}=\frac{1}{2N\rho k_BT}\int_0^P dP\left[1-k_BT\left[\frac{\partial\rho}{\partial P}\right]_{N,T}\right]^2. \tag{17}$$

Given the equation of state along an isotherm, this equation can be used to calculate explicitly ΔF_N. Once these corrections are calculated, Eq. (16) can be used to compute $\Delta\mu_N$. Finite-size corrections to the pressure can be calculated by recalling that $P=-(\partial F/\partial V)_{N,T}$. After some straightforward algebra, it follows that

$$\Delta P_N(\rho)=k_BT\rho^2\frac{\partial}{\partial\rho}\left[\frac{\Delta F_N(\rho)}{Nk_BT}\right]. \tag{18}$$

In Fig. 5 we compare the simulation predictions for the finite-size corrections to the free energy in the isotropic phase $\Delta F_N^{\rm sim}$ with the corresponding theoretical predictions obtained from Eq. (17) for each value of N in the range of densities considered in this work. The integration in Eq. (17) was performed for each value of N by considering the equations of state as obtained from simulation. In each case, $(\partial\rho/\partial P)_{N,T}$ was obtained from a cubic spline. The theoretical finite-size corrections to the chemical potential and pressure in the isotropic phase were calculated by using Eqs. (14) and (16). Comparison with simulation is shown in Figs. 6 and 7.

These figures show that the system-size effects predicted by Eqs. (15)–(17) considerably underestimate the corresponding values found from simulation. It should be noticed that the difference is both quantitative as well as qualitative. Inspection of Fig. 5 shows that Eq. (17) predicts a monotonic increase of ΔF_N, with density. However, the simulation results indicate quite a different behavior for ΔF_N: a maximum is achieved at $\rho^*\approx0.25$, followed by a sudden decrease. This qualitative difference between theoretical predictions and simulation are also displayed by the corrections to the chemical potential and pressure, as observed in Figs. 6 and 7. In these cases, the simulation results show that finite-size corrections are even negative in the isotropic side of the isotropic-nematic transition ($0.25<\rho^*<0.32$), while the predictions from Eqs. (15) and (17) are positive at all densities. If we recall the behavior of the order parameter (see Fig. 1), we can tentatively ascribe the existence of negative corrections to the large nematic fluctuations below the transition. To understand this point further, let us consider two system sizes N_1 and N_2 such that $N_1<N_2$. In the isotropic phase but far from the transition we expect the order parameter to behave as $S_2(N_2)<S_2(N_1)$. In this region, where the nematic fluctuations are negligible, the difference in order parameter values are exclusively due to the N dependence exhibited by S_2 [$S_2(N)\sim N^{-1}$]; furthermore, the pressure of the system is expected to be $P(N_2)<P(N_1)$ and hence the finite-size corrections are expected to be positive. In the pretransition region, where nematic fluctuations are noticeable, we still expect smaller order parameter values for larger system sizes, but now $S_2(N_2)\ll S_1(N_1)$. Larger systems still retain the isotropiclike behavior while under the same conditions smaller systems behave closer to a nematiclike phase. As a consequence, $P(N_2)>P(N_1)$ and in this region we would find negative corrections to finite size. This effect, entirely due to the peculiar nature of a weak first-order transition, is not included in Eqs. (15)–(17) and hence, the discrepancy between simulation and theory should not be surprising.

We have not tried to make use of Eqs. (15)–(17) in the nematic phase because the propagation of errors make the comparison with the simulation results meaningless.

V. CONCLUDING REMARKS

In this paper we have studied the influence of finite size in the simulation of a molecular fluid modeled by the Gay-Berne potential. The fluid is shown to exhibit a weak first-order isotropic-nematic transition for systems of 256 molecules. During this work, we have shown that the nematic phase is still stable when larger systems are considered. By using thermodynamic integration along an isotherm, we have located the transition densities for each system size. We should emphasize that this method appears to work properly even for such a weak transition. However, it should be mentioned that its implementation requires simulation at many intermediate state points far from the region of interest. This turns out to be quite time consuming. It would be desirable to resort to other direct methods for locating the phase transition. A possible alternative route would be to monitor the density distribution function for the order parameter $P_N(S_2)$. As noted elsewhere (see, for instance, Ref. [2]), $P_N(S_2)$ develops a double-peak structure close to the transition which allows the location of the transition (in the literature what is rather recorded is the energy probability distribution function [5,21]). Even though this procedure implies

very long runs to record $P_N(S_2)$ with great accuracy, it has the advantage that few runs in the region of interest would be enough for determining the transition. Work in this direction is presently in progress.

We have shown that the isotropic-nematic transition shifts to slightly higher densities with increasing system size. It is argued that the transition densities seem to scale as N^{-1}. By using this scaling behavior we have obtained the transition densities in the infinite-size limit. The transition retains its first-order nature with increasing N, although the density jump at the transition gets smaller as $N \to \infty$.

System-size effects have been analyzed in the isotropic and nematic sides of the transition. Comparison between system-size corrections as obtained from computer simulation has been made with theoretical predictions of the N dependence of thermodynamic properties of the system. It has been shown that the theoretical approximation underestimates the simulation corrections. Moreover, there are qualitative difference in the dependence of these corrections on the reduced density of the fluid. It has been argued that the negative corrections found in simulation for the pressure and chemical potential can be associated with the large nematic fluctuations found in the pretransition region.

ACKNOWLEDGMENTS

We wish to acknowledge M. P. Allen, L. F. Rull, and G. Jackson for useful comments and discussions and for their critical reading of the manuscript. Allocation of computer time at the Centro Informático Científico de Andalucía is gratefully acknowledged. This research was supported by the DGICYT of Spain under Grant No. PB-89-640.

[1] M. N. Barber, in *Phase Transitions and Critical Phenomena,* edited by C. Domb and J. L. Lebowitz (Wiley, New York, 1983), Chap. 2.

[2] O. Mouritsen, in *Computer Studies of Phase Transitions and Critical Phenomena* (Springer-Verlag, Berlin, 1984).

[3] V. Privman, in *Finite Size Scaling and Numerical Simulation of Statistical Systems,* edited by V. Privman (World Scientific, Singapore, 1990), Chap. 1.

[4] V. Privman and M. E. Fisher, J. Stat. Phys. **33**, 385 (1983); D. P. Landau, in *Finite Size Scaling and Numerical Simulation of Statistical Systems* (Ref. [3]), Chap. 5; C. Borgs and R. Kotecky, Phys. Rev. Lett. **68**, 1734 (1992).

[5] M. S. S. Challa, D. P. Landau, and K. Binder, Phys. Rev. B **34**, 1841 (1986).

[6] B. Guillot and Y. Guissani, Mol. Phys. **54**, 455 (1985).

[7] U. Heinbuch and J. Fisher, Mol. Simul. **1**, 109 (1987).

[8] B. Smit and D. Frenkel, J. Phys.: Condens. Matter **1**, 8659 (1989).

[9] G. J. Zarragoicoechea, D. Levesque, and J. J. Weis, Mol. Phys. **75**, 989 (1992).

[10] D. Frenkel and B. M. Mulder, Mol. Phys. **55**, 1171 (1985).

[11] C. Zannoni, in *The Molecular Physics of Liquid Crystals,* edited by G. R. Luckhurst (Academic, New York, 1979), Chap. 9; U. Fabbri and C. Zannoni, Mol. Phys. **58**, 763 (1986).

[12] E. de Miguel, L. F. Rull, M. K. Chalam, K. E. Gubbins, and F. van Swol, Mol. Phys. **72**, 593 (1991).

[13] J. G. Gay and B. J. Berne, J. Chem. Phys. **74**, 3316 (1981).

[14] D. J. Adams, G. R. Luckhurst, and R. W. Phippen, Mol. Phys. **61**, 1575 (1987).

[15] E. de Miguel, L. F. Rull, M. K. Chalam, and K. E. Gubbins, Mol. Phys. **74**, 405 (1991); M. K. Chalam, K. E. Gubbins, E. de Miguel, and L. F. Rull, Mol. Simul. **7**, 357 (1991).

[16] For a recent review, see D. Frenkel, in *Computer Simulation in Materials Science,* Vol. 205 of *NATO Advanced Study Institute Series E: Applied Sciences,* edited by M. Meyer and V. Pontikis (Kluwer, Dordrecht, 1991), p. 85.

[17] G. R. Luckhurst and P. Simpson, Chem. Phys. Lett. **95**, 149 (1983).

[18] M. P. Allen and D. J. Tildesley, in *Computer Simulation of Liquids* (Clarendon, Oxford, 1987).

[19] R. Eppenga and D. Frenkel, Mol. Phys. **52**, 1303 (1984).

[20] W. H. Press, B. P. Flannery, S. A. Teukolsky, and W. T. Vetterling, in *Numerical Recipes* (Cambridge University Press, Cambridge, 1986).

[21] M. P. Allen, Mol. Simul. **4**, 61 (1989); C. Borgs and W. Janke, Phys. Rev. Lett. **68**, 1738 (1992).